2018 24th International Conference on Pattern Recognition (ICPR)
Beijing, China, August 20-24, 2018

Convolutional Features-Based CRF Graph Matching for Tracking of Densely Packed Cells

Weili Qian, Yangliu Wei, Xueping Wang, and Min Liu*
College of Electrical and Information Engineering
Hunan University
Changsha, China
E-mail: liu_min@hnu.edu.cn

***Abstract*—The tracking of plant cells across large-scale microscopy image sequences is very challenging, because plant cells are densely packed in a specific honeycomb structure, and the microscopy images can be randomly translated, rotated and scaled in the imaging process. This paper proposes a convolutional features-based conditional random field (CRF) graph matching method to track plant cells in unregistered image sequences, by exploiting deep features extracted from deep convolutional neural networks and tight spatial topology feature of neighboring cells as contextual information. Because the extracted convolutional feature and spatial topology feature are resilient to image translation, rotation and scaling, the proposed CRF matching approach is able to track plant cells across unregistered image sequences. Compared with other plant cell tracking methods, the experimental results show that the proposed method improves the tracking accuracy rate by about 30% in the unregistered cell image sequences.**

Keywords—cell tracking; conditional random field; convolutional features; microscopy image sequences

I. INTRODUCTION

Exploring the causal relationship of cell growth patterns and motion characteristics is the basis for the biomedical research of cell behavior. The subject of this study, the shoot apical meristems (SAMs) also referred to as the stem-cell niche, is the most important part of the plant body because it supplies cells for all the above ground plant parts such as leaves, branches and stem, and at the same time maintains its stable size. The analysis of the plant cell images, such as cell tracking, is very critical for the modeling of plant cell growth pattern and gene expression dynamics. The development of fully automated image analysis pipelines for large volume plant cell image data is becoming necessity.

There has been some work on automated tracking of cells in time-lapse images for both plants and animals [1-10]. However, tracking methods for animal cells and other regular objects are difficult to be adapted to track the plant cell population with a special honeycomb structure in microscopic image sequences, for several reasons: (1) plant cells are densely packed in a specific honeycomb structure, where they are in close contact with each other and share very similar physical features; (2) plant cells are dividing along time; (3) the microscopy images can be translated, rotated and scaled in the imaging process, as shown in Fig.1 (d). In order to track the plant cells, Fernandez et al. [11] developed an automated image processing pipeline for SAM cells, but their image data are acquired from multiple angles, which imposes a limitation on the temporal resolution of the image series.

In the earlier studies, a 2D local graph matching method was proposed in [12, 13] to track plant SAM cells. In such framework, every cell is represented by a vertex in the graph and the neighboring vertices are connected by an edge. The local graph structure automatically includes the relative position information of the cells, such as the distance between two neighboring cells (edge length) and edge orientation. It successfully exploits the cells' local neighboring structure to match the plant cells, and the experimental results have confirmed the effectiveness of the local graph matching method. However, the existing local graph matching algorithm requires registration of the microscopy image sequences. This will pose significant challenges to the efficient and robust tracking of plant cells in microscopy image sequences with inevitable random image translation, rotation and scaling in the imaging process, as shown in Fig. 1 (d).

Recently, deep learning based features have demonstrated state-of-the-art results on a wide range of visual recognition and tracking tasks [14-17]. As one of the most effective deep learning approaches, convolutional neural network, which consists of convolutional (Conv), pooling (Pool), inception module, normalization layer and fully-connected (Fc) layers, as shown in Fig. 3 (A), has already demonstrated remarkable performance on benchmark datasets such as ImageNet [18]. Because the convolutional features is translation invariant, scaling invariant and rotation invariant within a certain range, in this paper, we propose to extract CNN features using the VGG-Net [19], which is trained on the large-scale ImageNet dataset [18] with category-level label, to track plant cells.

As confirmed in the local graph matching method [12, 13], the cells' contextual information is the most discriminating feature, in this paper, we propose to embed the deep convolutional features and topology feature of neighboring cells within a conditional random field framework, which is a perfect probabilistic framework for labeling sequential data

*Min Liu is the corresponding author. This work was supported by the National Natural Science Foundation of China (Grant Nos. 61771189 and 61301254).

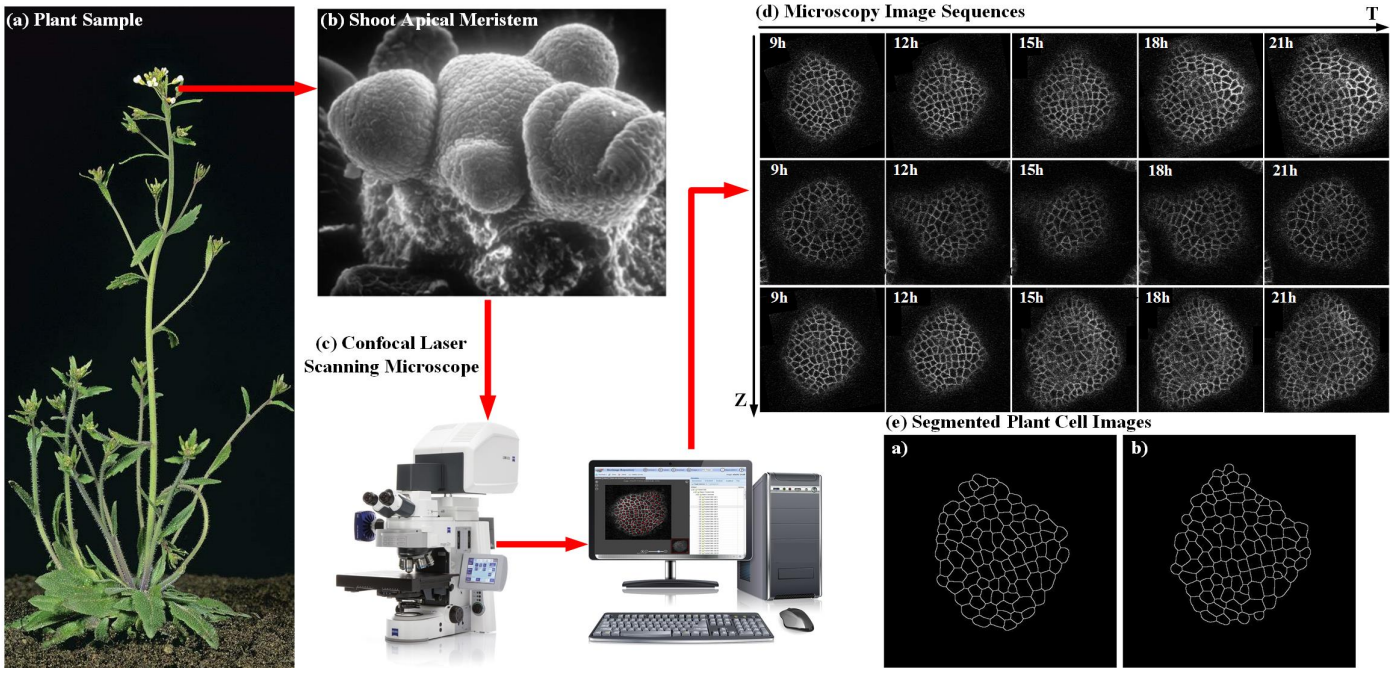

Fig. 1. The plant cell microscopy image sequences: (a) A plant sample; (b) Shoot apical meristem; (c) Confocal Laser Scanning Microscope; (d) Microscopy image sequences; (e) The segmented images by watershed method.

based on a conditional approach described in [20, 21]. Because the extracted convolutional feature and spatial topology feature are resilient to image translation, rotation and scaling, the proposed CRF graph matching algorithm is able to track plant cells across unregistered image sequences. The pipeline of the proposed convolutional features-based conditional random field graph matching method for plant cell population is shown in Fig. 2. The proposed method will grow the cell correspondence from the most similar cell pair (known as the "Seed Pair") with the least CRF potential. Starting from the "Seed Pair", similarly, in each correspondence growing process, it tends to match the most reliable cells with the least CRF potential from the tracked cells' neighboring cells.

The rest of the paper is organized as follows. The detailed methodology is given in Section II. We have shown the experimental results and validation of our approach in Section III followed by conclusion in Section IV.

II. Detailed Methodology

A. Watershed segmentation

The input to our plant cell tracking system is microscopy images across multiple time points. Watershed transformation is used to segment the plant cell boundaries [22]. It treats the input image as a continuous field of basins (low-intensity pixel regions) and barriers (high-intensity pixel regions), and outputs the barriers that represent plant cell boundaries. The experimental results in a previous work have confirmed the effectiveness of the watershed segmentation approach for plant cells [22]. Examples of segmented plant cells by watershed transformation method can be found in Fig. 1 (e). The convolutional features are extracted within the region of each segmented cells, as introduced below.

B. Convolutional Features

It has been confirmed that the activations of the convolutional layers in CNN networks can be exploited as effective image features for object recognition and tracking [14-17]. In this paper, we propose to obtain convolutional features for plant cells by extracting the activations of multiple convolutional layers through pre-trained CNN networks, e.g., VGG-Net [19].

Along with the CNN forward propagation, the semantical discrimination between objects (plant cells in our work) from different categories is strengthened, while the spatial resolution for precise localization is gradually reduced. For plant cell tracking, we are interested in accurate locations of a target cell. So the fully-connected layers are ignored as they show little spatial resolution, i.e., 1×1. Besides, due to the pooling operators used in the CNNs, spatial resolution is gradually reduced with the increase of the depth of convolutional layers. For example, the convolutional feature maps of pool5 in the VGG-Net are of spatial size 7×7, which is $1/32$ of the input image size 224×224. For visual object tracking, such low spatial resolution is insufficient to locate targets accurately. This issue is alleviated by resizing each feature map to a fixed larger size with bilinear interpolation instead [14].

Specifically, let us assume the pre-trained CNN network contains S convolutional layers, and $C^s(s=1,2,...,S)$ represents the feature maps of the s-th convolutional layer. The size of C^s is $w_p^s \times h_p^s \times c^s$, where c^s represents the number of feature channels in the s-th convolutional layer, w_p^s and h_p^s represent the width and height of the p-th channel of the

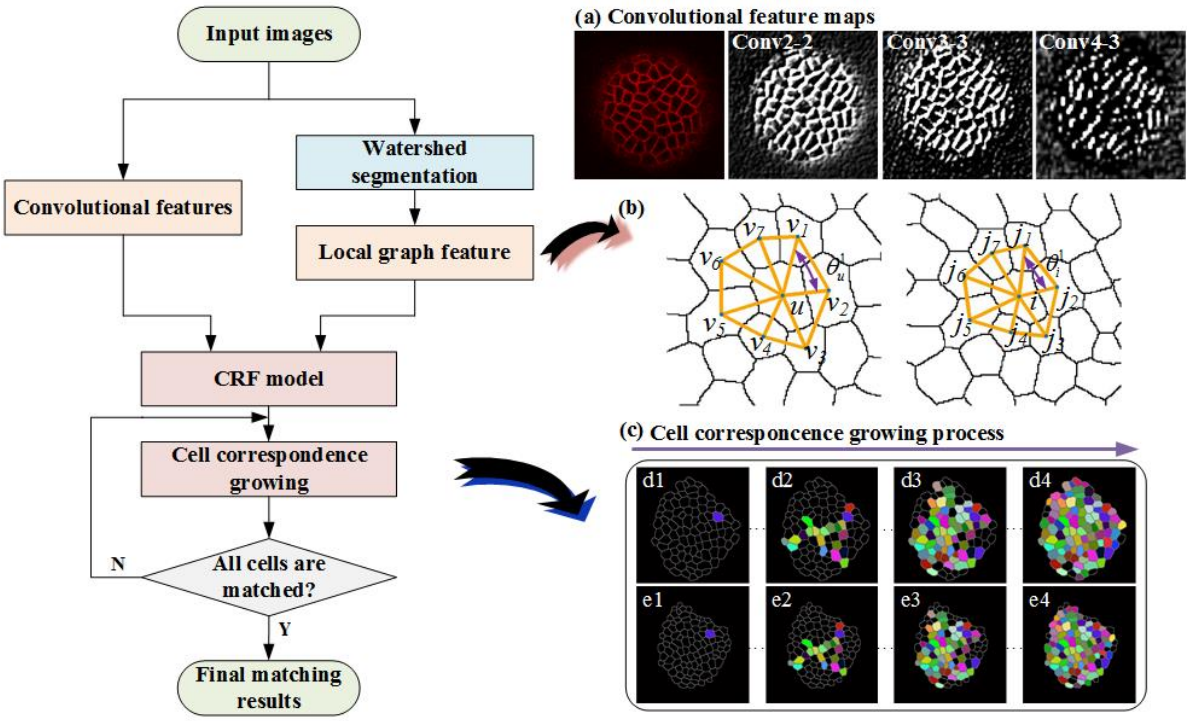

Fig. 2. The pipeline of the proposed convolutional features-based CRF graph matching method for plant cell population.

channel ($p = 1, 2, ..., c^s$), respectively. Because the size of feature maps in different convolutional layers is different, every feature map is upsampled by the bilinear interpolation [14]. The upsampled outputs from the feature map in the 10-th of the conv2-2, conv3-3 and conv4-3 layers are illustrated in Fig. 3 (B). We can clearly see that features on the conv2-2, conv3-3 and conv4-3 layers are effective in discriminating between different plant cells and the background.

For each segmented cell i, the convolutional features are extracted from the outputs of the interpolated feature map within the segmented region of i. The extracted convolutional features in the 10-th channel of the conv2-2, conv3-3 and conv4-3 layers for a given cell are illustrated in Fig. 3 (b)-(d).

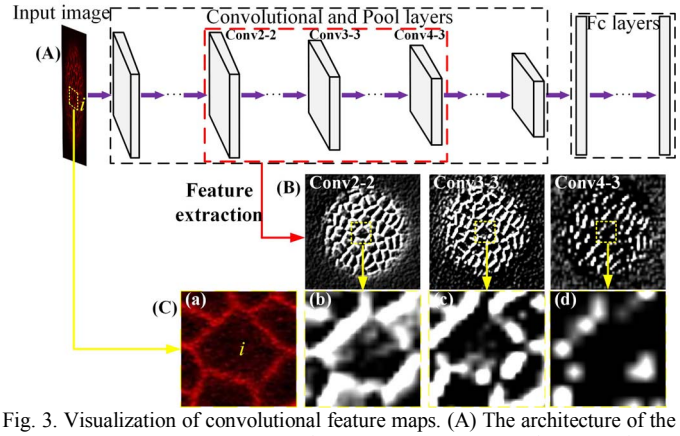

Fig. 3. Visualization of convolutional feature maps. (A) The architecture of the VGG-16. (B) Features are extracted on conv2-2, conv3-3 and conv4-3 layers using the VGG-16. (C) (a) is the enlargement of the central region denoted in the input image, (b)-(d) are the enlargements of the central regions denoted in conv2-2, conv3-3 and conv4-3.

C. Local Graph

After segmentation, every cell is represented by a vertex and neighboring vertices are connected by an edge. As shown in Fig. 4 (b), neighborhood set $\mathcal{N}_i$ of a cell i contains the set of cells that share a boundary with i. Thus, every graph consists of a cell i and a set of clockwise ordered neighboring cells. The ordering of the cells in $\mathcal{N}_i$ is important because under non-reflective similarity transformation, the absolute positions of the neighboring cells could change but the cyclic order of the cells remains invariant.

D. CRF Model for Cell Tracking

1) CRF Based Graph

In this paper, the plant cell tracking problem is formulated as a cell labeling problem, the solution of which is relied on the CRF framework [23]. As in the graphical model shown in Fig. 4, the sites in $\mathcal{S}$ are related to one another via a neighboring system, which is defined as $\mathcal{N} = \{\mathcal{N}_i, i \in \mathcal{S}\}$, where $\mathcal{N}_i$ are neighboring cells of the central cell i. Given the confocal plant cell images I_X and I_Y, the observation O is defined as the set of $I_X \bigcup I_Y$, X is the cell label in image I_X and Y is a random variable over corresponding label sequences. Then the CRF formulation is expressed as

$$P(Y|X) = \frac{1}{Z}\exp(-E(Y,X)) \qquad (1)$$

Where Z is the normalization factor that does not depend on Y, $E(Y|X)$ is a potential function as below,

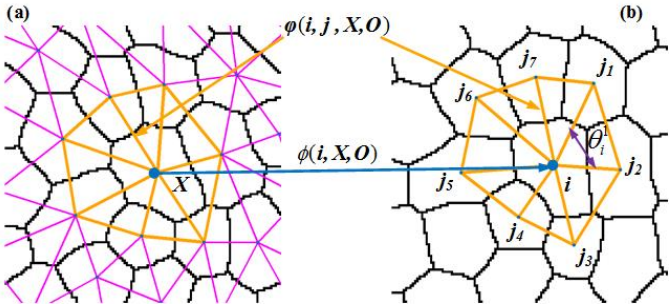

Fig. 4. Local graphs in two adjacent images. The unary potential $\phi(i,X,O)$ is defined on every node of the graph. (a) and (b) illustrate the second order potential $\varphi(i,j,X,O)$.

$$E(Y,X)=\sum_{i\in\mathcal{S}}\phi(i,X,O)+\sum_{i\in\mathcal{S}}\sum_{j\in\mathcal{N}_i}\varphi(i,j,X,O) \qquad (2)$$

The unary potential $\phi(i,X,O)$ is based on the feature similarity of the central cell pair, and the second order potential $\varphi(i,j,X,O)$ is based not only on the central cell pair but also the adjacent cells. The computation of unary potential and second order potential is introduced below.

2) Feature Functions

a) Computation of unary potential: The unary potential $\phi(i,X,O)$ is defined on every node of the graph and is the likelihood on the label given the observation O . This potential is computed independently between the convolutional features of a given cell node pair.

Let $d^i_{s,p}$ denotes the p-th channel feature map in the s-th convolutional layer of the cell i in image I_X , and $d^u_{s,p}$ denotes the p-th channel feature map in the s-th convolutional layer of the cell u in image I_Y . The correlation between the features gives us a distance measure between cells i and u . In this paper, the convolutional features are only extracted on conv2-2, conv3-3 and conv4-3 layers, thus the unary potential between cells i and u is expressed as

$$\phi(i,u)=\sum_{s=2}^{4}\sum_{p=1}^{c^s}\frac{\lambda_{s-2}}{c^s}\cdot\frac{1}{d^u_{s,p}\otimes d^i_{s,p}} \qquad (3)$$

The normalization parameters λ_1, λ_2 and λ_3 in Eq. (3) are learnt from a training dataset.

b) Computation of second order potential: The second order potential function is defined on edges that connect pairs of neighboring nodes. Its computation relies on the cells' local graph features. Essentially, if cell i is matched to cell u , then the relative position of cell i with respect to its neighboring cell j should be very similar to the relative position of cell u with respect to its neighboring cell v. Let us define the cell i in slice I_X with its neighboring cells $\mathcal{N}_i=\{j_1,j_2,...,j_m\}$ and let us define cell u in the next slice I_Y with its neighboring cells $\mathcal{N}_u=\{v_1,v_2,...,v_n\}$. m and n are the number of neighbors for cells i and u respectively. If $m\neq n$, that means cells i and u are not the corresponding cell pair, so we assign a large value to the second order potential φ .

Let θ^k_i denotes the angle between edges connecting cell i and its neighboring cells j_k , j_{k+1} , $(k=1,2,...,m-1)$, as shown in Fig. 4 (b), θ^m_i denotes the angle between edges connecting cell i and its neighboring cells j_m , j_1 . Similarly, θ^k_u denotes the angle between edges connecting cell u and its neighboring cells v_k , v_{k+1} , $(k=1,2,...,m-1)$, θ^m_u denotes the angle between edges connecting cell u and its neighboring cells v_m , v_1 . In this paper, the second order CRF potential is defined as the difference of the angles in the local graphs for cell pair (i,u) .

To ensure that the second order potential takes care of the rotation of the local graph, we consider all cyclic permutations of the clockwise ordered neighbor set $\{\mathcal{N}_i^1,\mathcal{N}_i^2,....\mathcal{N}_i^m\}$ of the cell i in image I_X . The cyclic permutations of the set $\{x_1,x_2,....x_m\}$ can be written in terms of the shift q $(q=0,1,...,(m-1))$ as the set $\{x_{(1+q-1)_{\mathrm{mod}(m)}+1},x_{(2+q-1)_{\mathrm{mod}(m)}+1},...,x_{(m+q-1)_{\mathrm{mod}(m)}+1}\}$. As an example, if $(1,2,3)$ is the given sequence, then possible values of the shift $q=0,1,2$ and all the cyclic permutations of the sequence $(1,2,3)$ will be $(1,2,3),(2,3,1),(3,1,2)$ for $q=0,1,2$ [24]. We consider all cyclic permutations of the clockwise ordered neighbor set $\{\mathcal{N}_i^1,\mathcal{N}_i^2,....\mathcal{N}_i^m\}$ of the cell i in image I_X and define $\varphi(i,u)$ as the minimum distance between two cells i and u based on all permutations.

For $q\in\{0,1,...,m-1\}$, we compute the summation of angle differences of i and u in the local graphs for each permutation q ,

$$D(i,u;q)=\sum_{k=1}^{m}(\theta^r_i-\theta^k_u),\quad r=(k+q-1)_{mod(m)}+1 \qquad (4)$$

Then the minimum of $D(i,u;q)$ is picked as the second order potential as

$$\varphi(i,u)=\omega\cdot\min D(i,u;q) \qquad (5)$$

The normalization parameter ω in Eq. (5) is learnt from a training dataset.

3) Parameter Estimation and Inference

We describe how to estimate the parameters $\theta=\{\lambda,\omega\}$, $\lambda=\{\lambda_1,\lambda_2,\lambda_3\}$ of potentials in a CRF. Given a subset $\{x^{(t)},y^{(t+1)}\}_{t=1}^{T}$ from our dataset with ground-truth. $x^{(t)}=\{x_1^{(t)},x_2^{(t)},\cdots,x_r^{(t)}\}$ is a sequence of cells as the input and $y^{(t+1)}=\{y_1^{(t+1)},y_2^{(t+1)},\cdots,y_r^{(t+1)}\}$ is the sequence of the matching results. In the learning process, we want to pick the values for

$\theta = \{\lambda, \omega\}$ that would maximize the conditional log-likelihood of the CRF on the training sequences, as below,

$$L(\theta) = \prod_{t=1}^{T} P(y^{(t+1)} \left| x^{(t)}, \theta \right.) \quad (6)$$

$$(\bar{\theta}) = \arg\max_{(\lambda,\omega)} (L(\theta)) \quad (7)$$

The gradient ascent approach is used to solve the parameter optimization problem. Given the above CRF model and its learned parameters, we use an inference approach based on the Loopy Belief Propagation [25, 26] to find the cell label y' that is most likely to maximize the conditional probability of Eq. (1), as below,

$$y' = \arg\max_{y} (P(y \left| x \right.)) \quad (8)$$

4) CRF Graph Based Cell Matching

Similar to the local graph matching algorithm presented in the previous work [12], our proposed CRF graph matching based tracking strategy is to first find the most similar cell pair (Seed Pair) with the least CRF potential, and then we grow the cell correspondence spatially from the Seed Pair.

Besides, a dynamically changing second order potential is employed in the cell correspondence growing process, because the cells that have been matched already are not going to be included in φ. Assume $M_1, M_2 \cdots$ and M_w are the cells which have already been matched till the current iteration, and $M = M_1 \bigcup M_2 \bigcup \cdots \bigcup M_w$. We use a ranked CRF graph based matching scheme to choose the cell pair with the least potential in the cell neighboring system $\mathcal{N}_M$, where $\mathcal{N}_M = \mathcal{N}_{M_1} \bigcup \mathcal{N}_{M_2} \bigcup \cdots \bigcup \mathcal{N}_{M_w}$. Our proposed CRF graph matching algorithm will continue to find all possible cell matches using this cell correspondence growing scheme.

III. Experimental Results

We have tested our proposed cell tracking method on multiple plant SAM datasets. The experimental results are demonstrated on plant cell image sequences which are captured by a confocal laser scanning microscope, across consecutive time instants with a time interval of 3 hours between two consecutive instants. Some of them are registered image sequences and some of them are unregistered image sequences. The algorithm is implemented using MATLAB on a PC with 3.3-GHz CPU and 4-GB memory, and using the Caffe framework [27].

The convolutional features are extracted using the VGG-16 [19], which is trained on the large-scale ImageNet dataset [18] with category-level label. We first remove the fully-connected layers and use the outputs from the conv2-2, conv3-3 and conv4-3 convolutional layer as the convolutional features. The extracted convolutional features are illustrated in Fig. 3.

We first compare the plant cell tracking performance by using the convolutional features from different layers (c2, c3 and c4) of VGG-16. The tracking accuracies of the proposed method in registered image sequences and unregistered image sequences are shown in Fig. 5, by using convolutional features from single layer, and the combination of two layers (c2 and c3, c2 and c4, c3 and c4), and the combination of three layers (c2, c3 and c4). The experimental results in Fig. 5 confirmed that the combinatorial features of conv2-2, conv3-3 and conv4-3 layers achieves the best plant cell tracking performance, either in the registered image sequences or the unregistered image sequences.

Fig. 5. Tracking accuracy comparison by using convolutional features from a single layer (c2, c3, or c4), and the combination of two layers (c2 and c3, c2 and c4, c3 and c4), and the combination of three layers (c2, c3, and c4).

Fig. 6 is an example of the plant cell tracking results across registered microscopy image sequences (upper row) and unregistered microscopy image sequences (lower row), from 6hr to 18hr, by our proposed convolutional features-based CRF graph matching model. Here the same color denotes the same cell across different time instants. It is clearly seen that the plant cell population within the honeycomb structure are successfully tracked across multiple time points, even there are random translations, rotations and scaling.

In order to demonstrate the strength of the proposed convolutional features-based CRF graph matching model, we compared the tracking performance in the registered image datasets and unregistered image datasets, between the previous local graph matching model [12] (Previous) and the proposed method (Current) in Table I. By comparing the results in the 2nd and 3rd columns in Table I, we can clearly see that the proposed method reaches higher tracking accuracy than the previous local graph matching model in registered image datasets. By comparing the results in the 4th and 5th columns in Table I, we can see that the proposed method achieves much higher tracking accuracy in unregistered image datasets than the previous local graph matching model.

TABLE I. Tracking Accuracy Comparison

Dataset	Registered image sequences		Unregistered image sequences	
	Current	Previous [12]	Current	Previous [12]
A	93.12%	91.93%	92.31%	65.53%
B	91.98%	90.88%	91.87%	62.34%
C	90.18%	88.14%	89.84%	55.72%

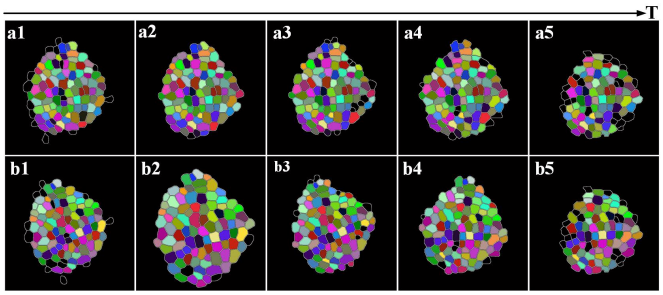

Fig. 6. The plant cell tracking results across microscopy image sequences (from 6hr to 18hr), by our proposed model. (a1)-(a5) denote the cell images with registration. (b1)-(b5) denote the cell images without registration. The cells in the same color across different time points represent the same cells.

IV. CONCLUSION

This paper proposes a convolutional features-based conditional random field (CRF) graph matching method to track the plant cells in microscopy image sequences, by exploiting convolutional features extracted from deep convolutional neural networks and tight spatial topology feature of neighboring cells as contextual information. The extracted convolutional features and spatial topology feature are resilient to image translation, rotation and scaling, therefore the proposed tracking approach is able to track plant cells either in registered image sequences or unregistered image sequences. The experimental results show that the proposed method significantly improves the tracking accuracy, in plant cell microscopy image sequences with or without registration.

ACKNOWLEDGMENT

The authors would like to thank Prof. Amit Roy-Chowdhury from the Department of Electrical Engineering and Prof. Venugopala Reddy from the Department of Botany and Plant Sciences at the University of California, Riverside for offering insightful suggestions on building the proposed plant cell tracking framework.

REFERENCES

[1] F. Amat, W. Lemon, D. P. Mossing, K. McDole, Y Wan, K. Branson, E.W. Myers, and P.J. Keller, "Fast, accurate reconstruction of cell lineages from large-scale fluorescence microscopy data," Nat. Methods, vol. 11, no. 9, pp. 951-958, 2014.

[2] K. E. G. Magnusson, J. Jaldén, P. M. Gilbert, and H. M. Blau, "Global linking of cell tracks using the Viterbi algorithm," IEEE Trans. Med. Imag., vol. 34, no. 4, pp. 911-929, 2015.

[3] C. Huang, S. Sankaran, D. Racoceanu, S. Hariharan, and S. Ahmed, "Online 3-D tracking of suspension living cells imaged with phase-contrast microscopy," IEEE Trans. on Biomed. Eng., vol. 59, no. 7, pp. 1924-1933, 2012.

[4] A. Santella, Z. Du, and Z. Bao, "A semi-local neighborhood-based framework for probabilistic cell lineage tracing," BMC Bioinformatics, vol. 15, no. 1, pp. 217, 2014.

[5] J. Berclaz, F. Fleuret, E. Turreted, and P. Fua, "Multiple object tracking using k-shortest paths optimization," IEEE Trans. Pattern Anal. Mach. Intell., vol. 33, no. 9, pp. 1806-1819, 2011.

[6] O. Dzyubachyk, W. Van Cappellen, J. Essers, W. Niessen, and E. Meijering, "Advanced level-set-based cell tracking in time-lapse fluorescence microscopy," IEEE Trans. Med. Imag., vol. 29, no. 3, pp. 852-867, 2010.

[7] A. Milan, S. Roth, and K. Schindler, "Continuous energyminimization for multitarget tracking," IEEE Trans. Pattern Anal. Mach. Intell., vol. 36, no. 1, pp.58-72, 2014.

[8] M. Liu, R. Gong, W. Chen, H. Peng, "3D neuron tip detection in volumetric microcopy images using an adaptive ray–shooting model," Pattern Recognition, vol. 75, pp. 263-271, 2018.

[9] M. Schiegg et al., "Graphical model for joint segmentation and tracking of multiple dividing cells," Bioinformatics, vol. 31, no. 6, pp. 948-956, 2014.

[10] A. Liu, K. Li, and T. Kanade, "A semi-markov model for mitosis segmentation in time-lapse phase contrast microscopy image sequences of stem cell populations," IEEE Trans. Med. Imaging, pp. 359-369, 2012.

[11] R. Fernandez, P. Das, V. Mirabet, E. Moscardi, J. Traas, J. L. Verdeil, G. Malandain, and C. Godin, "Imaging plant growth in 4D: robust tissue reconstruction and lineaging at cell resolution," Nature Methods, vol. 7, no. 7, pp. 547-553, 2010.

[12] M. Liu, A. Chakraborty, D. Singh, R. K. Yadav, G. Meenakshisundaram, G. V. Reddy, and A. K. Roy-Chowdhury, "Adaptive cell segmentation and tracking for volumetric confocal microscopy images of a developing plant meristem," Molecular Plant, vol. 4, no. 5, pp. 922-931, 2011.

[13] M. Liu, P. Xiang, and G. Liu, "Robust plant cell tracking using local spatial-temporal context," Neurocomputing, vol. 208, no. 10, pp. 309-314, 2016.

[14] C. Ma, J. B. Huang, X. Yang, and M. H. Yang, "Hierarchical convolutional features for visual tracking," in Proc. of ICCV, pp. 3074-3082, 2015.

[15] X. Lu, Y. Chen, and X. Li, "Hierarchical recurrent neural hashing for image retrieval with hierarchical convolutional features," IEEE Transactions on Image Processing, vol. 27, no. 1, pp.106-120, 2018.

[16] A. Babenko and V. Lempitsky, "Aggregating local deep features for image retrieval," in Proc. of ICCV, pp. 1269-1277, 2015.

[17] Y. Kalantidis, C. Mellina, and S. Osindero, "Cross-dimensional weighting for aggregated deep convolutional features," In Proc. of ECCV, pp. 685-701, 2015.

[18] J. Deng, W. Dong, R. Socher, L. Li, K. Li, and F. Li. "Imagenet: A large-scale hierarchical image database," In Proc. of CVPR, 2009.

[19] K. Simonyan and A. Zisserman. "Very deep convolutional networks for large-scale image recognition," in Proc. of ICLR, 2015.

[20] A. Chakraborty, A. K. Roy-Chowdhury, "Context aware spatio-temporal cell tracking in densely packed multilayer tissues," Medical Image Analysis, vol. 9, no. 1, pp. 149-163, 2015.

[21] M. Liu., Y. Wei, W. Qian, and H. Zhang, "Robust Plant Tracking in Noisy Image Sequences Using Optimal CRF Graph Matching," IEEE Signal Processing Letters, vol. 24, no. 8, pp.1168-1172, 2017.

[22] K. Mkrtchyan, D Singh, M. Liu, G. V. Reddy, A. K. Roy Chowdhury, and M. Gopi, "Efficient cell segmentation and tracking of developing plant meristem," in Proc. of ICIP, pp. 2165-2168, 2011.

[23] J. D. Lafferty, A. McCallum, and F. C. N. Pereira, "Conditional random fields: Probabilistic models for segmenting and labelingsequence data," in Proc. of ICML, pp. 282-289, 2001.

[24] K. Mkrtchyan, A. Chakraborty, A. K. Roychowdhury, "Optimal Landmark Selection for Registration of 4D Confocal Image Stacks in Arabidopsis," IEEE/ACM Trans Comput Biol Bioinform, vol. 14, no. 1, pp. 457-467, 2017.

[25] Y. Kong, M. Zhang and D. Ye, "A belief propagation-based method for task allocation in open and dynamic cloud environments," Knowledge-based Systems, vol. 115, pp. 123-132, 2016.

[26] K. P. Murphy, Y. Weiss Y, and M. I. Jordan, "Loopy belief propagation for approximate inference: An empirical study," in Proc. 15 Conf. Uncertainty Artif. Intell., pp. 467-475, 1999.

[27] Y. Jia, E. Shelhamer, J. Donahue, S. Karayev, J. Long, R. Girshick, S. Guadarrama, and T. Darrell, "Caffe: Convolutional architecture for fast feature embedding," in ACM international conference on Multimedia, pp. 675-678, 2014.